Do regional modifications in tissue mineral content and microscopic mineralization heterogeneity adapt trabecular bone tracts for habitual bending? Analysis in the context of trabecular architecture of deer calcanei

John G. Skedros,[1,2] Alex N. Knight,[1,2] Ryan W. Farnsworth[1] and Roy D. Bloebaum[1]

[1]*Bone and Joint Research Laboratory, Veterans Affairs Medical Center, Salt Lake City, Utah, USA*
[2]*Utah Orthopedic Specialists, Salt Lake City, Utah, USA*

Abstract

Calcanei of mature mule deer have the largest mineral content (percent ash) difference between their dorsal 'compression' and plantar 'tension' cortices of any bone that has been studied. The opposing trabecular tracts, which are contiguous with the cortices, might also show important mineral content differences and microscopic mineralization heterogeneity (reflecting increased hemi-osteonal renewal) that optimize mechanical behaviors in tension vs. compression. Support for these hypotheses could reveal a largely unrecognized capacity for phenotypic plasticity – the adaptability of trabecular bone material as a means for differentially enhancing mechanical properties for local strain environments produced by habitual bending. Fifteen skeletally mature and 15 immature deer calcanei were cut transversely into two segments (40% and 50% shaft length), and cores were removed to determine mineral (ash) content from 'tension' and 'compression' trabecular tracts and their adjacent cortices. Seven bones/group were analyzed for differences between tracts in: first, microscopic trabecular bone packets and mineralization heterogeneity (backscattered electron imaging, BSE); and second, trabecular architecture (micro-computed tomography). Among the eight architectural characteristics evaluated [including bone volume fraction (BVF) and structural model index (SMI)]: first, only the 'tension' tract of immature bones showed significantly greater BVF and more negative SMI (i.e. increased honeycomb morphology) than the 'compression' tract of immature bones; and second, the 'compression' tracts of both groups showed significantly greater structural order/alignment than the corresponding 'tension' tracts. Although mineralization heterogeneity differed between the tracts in only the immature group, in both groups the mineral content derived from BSE images was significantly greater ($P < 0.01$), and bulk mineral (ash) content tended to be greater in the 'compression' tracts (immature 3.6%, $P = 0.03$; mature 3.1%, $P = 0.09$). These differences are much less than the approximately 8% greater mineral content of their 'compression' cortices ($P < 0.001$). Published data, suggesting that these small mineralization differences are not mechanically important in the context of conventional tests, support the probability that architectural modifications primarily adapt the tracts for local demands. However, greater hemi-osteonal packets in the tension trabecular tract of only the mature bones ($P = 0.006$) might have an important role, and possible synergism with mineralization and/or microarchitecture, in differential toughening at the trabeculum level for tension vs. compression strains.

Key words: artiodactyl calcaneus; bone adaptation; bone mineral content; bone mineralization; cancellous bone; deer calcaneus; strain; trabecular bone.

Introduction

Determining the role that specific strain characteristics of the mechanical environment have in the attainment and maintenance of mechanically competent trabecular (cancellous) bone can be facilitated by the use of bones with simple, predictable loading. Lanyon (1974) introduced the artiodactyl (e.g. deer and sheep) calcaneus as a model for examining Julius Wolff's trajectorial theory of trabecular bone structures – the original conception of 'Wolff's law' as typically applied to the arched trabecular patterns in the proximal human femur (Skedros & Baucom, 2007; Skedros & Brand, 2011). Based on *in vivo* strains that were measured on the calcanei of walking animals, Lanyon's study demonstrates

Correspondence

John G. Skedros, M.D., Utah Orthopedic Specialists, 5323 South Woodrow Street, Suite 200, Salt Lake City, Utah 84107, USA. T: 801 713 0606; Fax: 801 713 0609; E: jskedros@utahboneandjoint.com
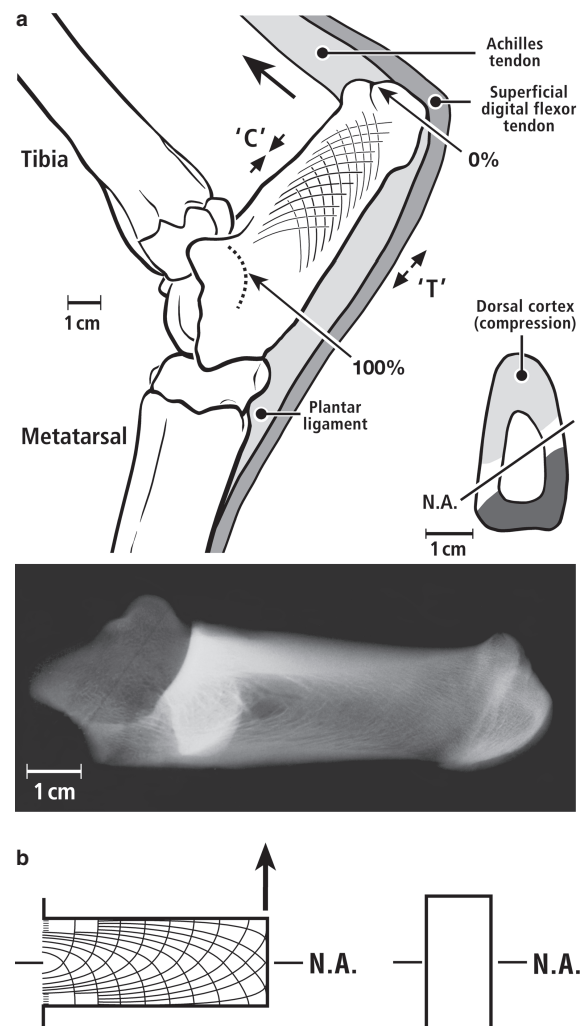
that this simple cantilevered beam-like bone can be generalized as an *in vivo* tension/compression model. These findings are consistent with general predictions of the trajectorial theory; namely, the direction of the principal compression and tension strains coincided with the direction of the dorsal and plantar trabecular bone tracts, respectively, as seen in lateral roentgenograms. Each trabecular tract therefore transmits stresses to and from its adjacent cortex (Fig. 1). Lanyon's (1974) findings have been corroborated *in vivo* in a study of the arched trabecular patterns in the potoroo calcaneus (Biewener et al. 1996). Additionally, the potential for trabecular re-alignment in accordance with changes in peak joint loading orientation has been verified experimentally (Pontzer et al. 2006; Barak et al. 2011).

Ex vivo studies of mule deer calcanei have advanced Lanyon's work by using seven strain gages per bone, including on the plantar 'tension' cortex (Su et al. 1999). These studies more clearly show that during physiological weight-bearing activities (including > 80% of stance phase during controlled ambulation), the calcaneal shaft behaves like a short-cantilevered beam with longitudinal compression and tension strains predominating on opposing dorsal and plantar cortices, respectively.[1] This strain distribution is highly consistent, even with extreme off-axis loads that simulate accidental loading (Su, 1998).

Studies of the hierarchical structural and material organization of cortical bone of mule deer and sheep calcanei have provided a wealth of knowledge about adaptation for a bending load history (Skedros et al. 1994a,b, 2001, 2004, 2007, 2009, 2011). The goal of these studies was to determine how structural and material variations might adapt the bone for regional differences in mechanical requirements and/or specific characteristics of the spatially non-uniform strain environment. These characteristics include the habitually prevalent/predominant longitudinal strain modes (e.g. tension and compression) and their associated strain magnitude differences, where the highest strains occur in the compression cortex during functional end-loading (Su et al. 1999; Lieberman et al. 2004). Results of these studies are broadly applicable to other limb bones because *in vivo* strain measurements have shown that various mammalian and avian bones typically experience directionally consistent bending (Lanyon & Baggott, 1976; Biewener & Bertram, 1993; Fritton & Rubin, 2001; Lieberman et al. 2004; Moreno et al. 2008; Skedros, 2011).

Fig. 1 (a) Lateral-to-medial view of the ankle region of a skeletally mature mule deer showing the calcaneus shaft 'length' and other associated bones. The trabecular patterns are stylized, and are based on the lateral-to-medial roentgenogram (at bottom). The distance from 0 to 100% was typically about 6.3 cm in the bones used in this study (range: 6.1 cm immature to 6.5 cm mature). The dotted line at the tip of the 100% arrow indicates the deeper location of the contour formed by the astragalus-calcaneus articular surfaces. The large dorsally directed arrow at the distal end of the bone indicates the direction of force imparted by the Achilles tendon (i.e. common calcaneal tendon) during mid-stance, placing the dorsal cortex in compression (converging arrows). The section at right is from 50% to 60% of the defined bone 'length', and shows the relatively thicker compression cortex. An approximate location of a theoretical neutral axis (NA) is shown. (b) The trabecular patterns of the artiodactyl calcaneus resemble stress trajectories of an idealized, homogeneous, isotropic cantilever subject to bending from a force (arrow) applied at the free (distal) end (redrawn from Currey, 1984, p. 140). The principal stress trajectories are diagrammatically represented; they were not drawn using mathematically derived coordinates (J.D. Currey, personal communication). The more crowded the trajectories, the greater the stress. The trajectories at the base of the cantilever have been omitted for clarity. The beam and a transverse cross-section of the beam show the location of the neutral axis (NA).

---

[1]For the purpose of clarity in discussing the results of the present investigation with results of past studies, the dorsal trabecular tract and dorsal cortex in most cases will be referred to as the 'compression' trabecular tract and 'compression' cortex, respectively, and the plantar trabecular tract and plantar cortex as the 'tension' trabecular tract and 'tension' cortex, respectively (Su et al. 1999; Skedros et al. 2004; Skedros & Baucom, 2007).

Compared with the 'tension' cortex, the opposing 'compression' cortex of skeletally mature mule deer calcanei has significantly greater cortical thickness, secondary osteon population density, cross-linked collagen and populations of compression-adapted osteon morphotypes (Gunasekaran et al. 1991; Skedros et al. 1994a,b, 1995, 2009). Porosity, fractional area of secondary osteonal bone, and preferred orientations of collagen fibers and mineral crystallites also markedly differ between these cortices (Skedros et al. 1994b, 2006, 2009). Finally, these calcanei have up to 11% greater mineral content (percent ash) in their 'compression' cortex than in their 'tension' cortex (Skedros et al. 1994a). This is the largest difference in mineralization that has been reported between regions of the same bone of any adult species. Relatively large mineral content differences have also been reported in the calcanei of mature North American elk (*Cervus elaphus*), horses and sheep (Skedros et al. 1997).

These previous studies of cortical bone of artiodactyl and perissodactyl calcanei stimulated the following question: Do 'tension' and 'compression' trabecular tracts exhibit important mineral content differences that are similar to their corresponding cortices? In this context it is important to point out that this modification would be expected in view of results from studies of bovine and human trabecular bone, which show that energy absorption to yield, and ultimate and yield strengths are nearly 30% lower for tension vs. compression loading (Keaveny et al. 1994a,b; Bayraktar et al. 2004). Similar disparities in mechanical behaviors in tension vs. compression have also been shown in human femoral cortical bone (Reilly & Burstein, 1975). If differences in mineral content that occur between the trabecular tracts in adult calcanei accommodate this disparity, then, similar to the nearby cortices, this would be expected to be a function of regional differences in remodeling rates (hemi-osteonal renewal in trabecular bone). If this plasticity in the adaptability of trabecular bone can be evoked, then the greater mineralization heterogeneity seen in the 'tension' cortex (when compared with the 'compression' cortex; Skedros et al. 1994b) might also be expected in the adjacent 'tension' trabecular tract.

It has been suggested in both cortical and trabecular bone that some degree of mineralization heterogeneity can be beneficial because it creates interfaces and microscopic modulus mismatches that optimize toughness and strength by accommodating microcrack formation and restricting microcrack propagation (Skedros et al. 2005; Wang & Niebur, 2006; Renders et al. 2008; Boskey et al. 2009; Ciarelli et al. 2009). However, recent studies have shown that in some circumstances (e.g. human aging/osteoporosis) greater mineralization heterogeneity can adversely affect mechanical properties of trabecular bone, including toughness (Busse et al. 2009; Bousson et al. 2011). We speculate that differences in 'beneficial' microscopic mineralization patterns and/or heterogeneity will be detected in comparatively young/healthy deer calcanei between the trabecular tracts as adaptations that accommodate the different mechanical requirements in tension vs. compression. It has been hypothesized that a similar difference in mineralization level and/or heterogeneity occurs between the superior 'tension' and inferior 'compression' trabecular tracts of the human femoral neck in young/healthy adults (Bloebaum et al. 2004; Loveridge et al. 2004; Lai et al. 2005). Advances in backscattered electron (BSE) imaging technology can now make detection of these differences possible in a model that does not show age or osteoporosis effects, and is also more clearly and simply loaded in bending than the proximal human femur. Experimental data in bovine trabecular bone demonstrating that microdamage accumulation is related to both trabecular architecture and loading history (Wang & Niebur, 2006) also support the possibility that natural selection mechanisms would favor adapting individual trabeculae differently in habitual tension vs. compression environments. In these clinical and basic science perspectives, the deer calcaneus is a useful model for investigating these possibilities.

The main purpose of this study is to quantify the bulk tissue mineral content (expressed as percent ash) and microscopic mineralization of the 'compression' and 'tension' trabecular and cortical regions of skeletally immature and mature deer calcanei. For the reasons stated above, we hypothesize that: first, the compression tract will have greater mineral content than the tension tract; and second, these mineral content differences will be correlated with differences in microscopic mineralization patterns and/or heterogeneity (quantified from BSE images). Because trabecular architectural variations are considered as the prominent means for accommodating mechanical requirements in tension vs. compression (Keaveny et al. 1994b, 2001; Kreider & Goldstein, 2009; Tassani et al. 2011), subsets of bones are also analyzed using micro-computed tomography (micro-CT) in order to identify potential differences in the adaptation of specific architectural characteristics between the tracts.

Materials and methods

Bones and specimen preparation

One left calcaneus was obtained from each of 30 male Rocky Mountain mule deer (*Odocoileus hemionus hemionus*) that had been indiscriminately selected from a sample of over 1000 wild animals that had been taken to a game processing facility during a hunting season (Northern Utah, USA Figs 1 and 2). Using the criteria of Purdue (1983), the distal growth plates (near the free end) of the calcanei were examined and the bones were divided into two groups: skeletally immature (*n* = 15; 1–2 years old) and skeletally mature (*n* = 15; 3–4 years old). Because the periosteal ('velvet') covering of the antlers had been shed and antler growth was complete, the relatively minor amount of appendicular cortical bone that had been reabsorbed for the

demands of antler growth would have been replenished (Banks et al. 1968; Hillman et al. 1973). Because the hunt was several weeks before the mating season, the animals had not yet participated in the aggressive physical interactions that are characteristic of the rut (Anderson, 1981; Goss, 1983). This diminishes the possibility that remodeling activities in this bone are secondary to systemic metabolic demands of antler growth and/or to the repair of bone microdamage caused during the rutting season.

Using methods described by Skedros et al. (1994a), the bones were manually cleaned, oriented and cut transversely at percentages of length. Sectioning produced segments that were 5–6 mm thick, corresponding to the 40% and 50% locations (Figs 1 and 2). The segments used in the present study are from what has been described as the 'pure beam' portion of the calcaneal shaft where relatively simple bending occurs (Skedros et al. 1994a).

Using a hollow drill bit, cylindrical cores (3 mm diameter) of cortical bone from the 'compression' and 'tension' aspects of each of the segments were removed under continuous water irrigation. Cores of trabecular bone were also obtained from the corresponding 'compression' and 'tension' trabecular tracts of each of the 40% and 50% sections (Figs 1 and 2).

Mineral content (percent ash) analysis

The cored specimens were thoroughly cleaned of marrow using a pulsatile water stream, defatted in full-strength reagent-grade chloroform under vacuum and constant stirring (16 days), and then dried to constant weight (4 days; < 0.05% change). Ashing was done at 600 °C for 24 h. Mineral content (percent ash) is expressed by dividing the weight of the ashed bone (W_{AB}) by the weight of the dried, defatted bone (W_{DB}) and multiplying this ratio by 100 [(W_{AB}/W_{DB})•100] (Skedros et al. 1993b).

BSE image analysis of mineralization level and heterogeneity

A transversely cut segment was obtained from the 50% shaft location of each of seven bones from each age group ($n = 7$ immature bones; $n = 7$ mature bones). These bones were different from those used for micro-CT analysis (see below), and were contralateral to those used for the analysis of bulk mineral content. These 14 segments were embedded in polymethyl methacrylate (PMMA; Emmanual et al. 1987). The surface of each PMMA-embedded 50% segment was ground, polished and carbon-coated (Cressington 208 high-vacuum carbon coater; Ted Pella, Redding, CA, USA). Digitized BSE images were obtained at 100 ×, 15 mm working distance, 20.0 kV accelerating voltage, −1.30 nA probe current, with four frames (0.84 × 1.13 mm wide) averaged (5 s per frame). The pixel resolution of the digital image was 1.2 square microns per pixel at 100 ×, with a resolution of 256 gray levels. Three BSE images were obtained in each trabecular tract in each bone, resulting in a total of 42 BSE images for each age group (21/dorsal tract, 21/plantar tract). Imaging sessions were calibrated using magnesium oxide (MgO) and aluminum oxide (Al_2O_3) standards (Skedros et al. 1993a).

Regional differences in mineralization were inferred from corresponding differences in the intensity of the image gray levels, where darker gray levels (lower numerical values) represent relatively lower mineralization, and brighter gray levels (higher numerical values) represent relatively higher mineralization

(Bloebaum et al. 1997). Gray level values in each BSE image are represented as integers from 0, 1, 2, 3, …, 255. These methods include the elimination of gray level values (gray level values ≤ 5) that represent tissue voids such as vascular canals and lacunae. Mineralization heterogeneity was measured as the full-width at half-maximum (FWHM) of the pixel gray level profile (Boskey, 2001; Ruffoni et al. 2007). This gray level profile is equivalent to the 'bone mineral density distribution' (BMDD) and other measures of mineralization heterogeneity described by others (Roschger et al. 1998; Bousson et al. 2001; Follet et al. 2004). Mean mineralization of the bone in each image was quantified as a weighted mean gray level (WMGL; Bloebaum et al. 1997).

Finally, the BSE images were randomly assorted without any identifying information, and the number of 'packets' were identified by JGS within the trabecular bone in each image (Ciarelli et al. 2003, 2009; Busse et al. 2009). 'Packets' refer to the basic structural units (typically hemi-osteonal bone) within trabecular bone (Parfitt, 1979; Ciarelli et al. 2009). Packets can be distinguished by being separated by cement lines and/or differences in the degree of lamellations (banding patterns) or mineralization; the latter is usually a function of mean tissue age (e.g. more highly mineralized bone correlates with age and/or reduced remodeling rate; Weinkamer & Fratzl, 2011). Trabecular bone packet prevalence was determined in order to identify differences in the amount of packets (per area of bone) between the compression and tension tracts in each age group. This prevalence is expressed as the number of packets divided by the absolute area of the trabecular bone in each image (osteocyte lacunae and vascular channels were included as part of the bone area).

Micro-CT analysis

Seven additional right (contralateral) calcanei (unembedded) from each age group, obtained from the same bone pairs used in the mineral content analyses, were scanned using a General Electric (GE) Medical Systems EVS-RS9 micro-CT scanner. Scanning parameters included 46.4 μm resolution, 80 kVp, 450 μA and 500 ms exposure time. All scans included cortical and trabecular bone. Regions of interest (ROI) were selected in the dorsal and plantar aspects of the 40% and 50% segments in the same regions where ashing was done in the contralateral bones. These ROIs were 4–5-mm-diameter cylinders that were aligned along the long axis of the bone and spanned the entire thickness of each 40% and 50% bone segment.

Quantitative analysis of most of the trabecular bone architectural characteristics in the ROIs was conducted with commercially available software (GE Health Care MicroView, version ABA 2.2). The eight parameters that were obtained included:

1 degree of anisotropy (DA; larger values reflect increased order/alignment of trabeculae);
2 bone volume fraction [BVF (%); bone volume ÷ total volume of ROI];
3 bone surface density [Bs/Bv (mm^{-1}), bone surface ÷ total volume of ROI];
4 trabecular thickness [Tb.Th (mm)];
5 trabecular spacing [Tb.Sp (mm), average trabecular separation];
6 trabecular number [Tb.N (no. mm^{-1})],
7 connectivity density [Conn.D (mm^{-3}), density of interconnected trabeculae]; and

8 structural model index (SMI; honeycomb-, rod- or plate-like trabeculae, as described below).

More detailed descriptions of these eight morphometric parameters can be found in prior studies (Hildebrand & Rueg-segger, 1997; Muller et al. 1998; Hildebrand et al. 1999; Fajardo & Muller, 2001; MacLatchy & Muller, 2002; Fajardo et al. 2007).

The SMI reflects the distribution of trabecular morphological types (Hildebrand et al. 1999; Fajardo et al. 2007): first, in an ideal plate-like structure the SMI value is 0; second, in an ideal rod-like structure the SMI value is 3 (Ding & Hvid, 2000); and third, negative SMI values represent very dense (low porosity) concave plate-like structures that resemble honeycombs, which are sometimes also referred to as spherical voids (Hildebrand et al. 1999; Stauber & Muller, 2006; Fajardo et al. 2007). The DA measures trabecular alignment along a preferred axis; at values close to 1 trabecular tissue is entirely isotropic (no preferred ori-entation), and as DA increases above 1 trabecular tissue becomes more anisotropic (trabeculae become more aligned; Fajardo & Muller, 2001). The DA was measured in 3-mm-diame-ter spheres using data measurements from the star volume dis-tribution (SVD) method (QUANT3D, IDL Virtual Machine, Boulder, Colorado, USA; Ryan & Ketcham, 2002; Ketcham & Ryan, 2004). The micro-CT measurements (made in pixels) were entered into the QUANT3D program as the 'user-entered sphere' ROI. For each of these ROIs, a quantitative iterative threshold method (Ridler & Calvard, 1878; Trussell, 1979) that determines gray-scale values based on the ROI was then employed (Ryan & Ketcham, 2002; Ketcham & Ryan, 2004; Maga et al. 2006; Fajardo et al. 2007; Ryan & Walker, 2010). For deter-mining SVD with dense vectors, the linear intercept was mea-sured for each ROI using 2049 uniformly distributed orientations with 4000 random rotation points (Ryan & Ketcham, 2002; Ketcham & Ryan, 2004; Hill & Richtsmeier, 2008). Using these volumes, DA was determined by methods described in previous studies (Odgaard et al. 1997; Ketcham & Ryan, 2004).
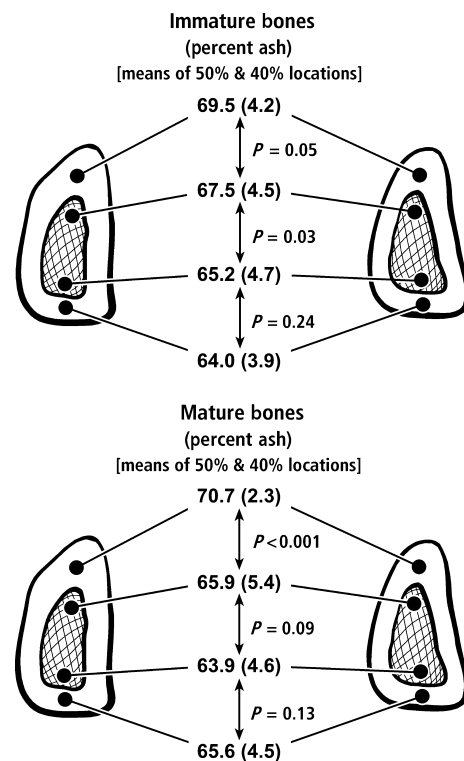
Statistical analysis

A two-factor analysis of variance (ANOVA) was conducted in terms of age (immature and mature) and location (dorsal and plantar trabecular tracts) between the two groups. Pair-wise compari-sons between the tracts were then assessed for statistical signifi-cance using Fisher's least significant *post hoc* test (Stat View Version 5.0, SAS Institute, Cary, NC, USA). When data sets devi-ated from normality, paired comparisons were evaluated with a Kruskal–Wallis *Z*-test (Hintze, 1995; Sokal & Rohlf, 1995). Paired *t*-tests were used to evaluate paired comparisons within each group for statistical significance. An alpha level of ≤ 0.05 is con-sidered statistically significant. Correlations were not conducted between micro-CT and mineralization data because they were not obtained from the same bones.

Results

Tension (plantar) and compression (dorsal) mineral content (percent ash) data

Results of mineral (percent ash) analyses are summarized in Fig. 2. Combined data (40% + 50% sections) of immature

Immature bones
(percent ash)
[means of 50% & 40% locations]
69.5 (4.2)
P = 0.05
67.5 (4.5)
P = 0.03
65.2 (4.7)
P = 0.24
64.0 (3.9)

Mature bones
(percent ash)
[means of 50% & 40% locations]
70.7 (2.3)
P < 0.001
65.9 (5.4)
P = 0.09
63.9 (4.6)
P = 0.13
65.6 (4.5)

Fig. 2 Diagrammatic depictions of the cut surfaces of the 40% and 50% segments showing *P*-values of selected paired comparisons of mineral content data (average values and standard deviations are shown). The dark circles indicate locations where the cylindrical bone cores were removed for mineral content analysis. In the trabecular bone, the dark circles also indicate the locations where micro-CT measurements were made. There are no significant differences (*P* < 0.05) between the age groups in terms of the tract comparisons (i.e. immature dorsal tract vs. mature dorsal tract). No attempt is made to show the age-related differences in size of the cross-sections.

bones show 3.6% greater mineral content in the 'compres-sion' vs. the 'tension' tract (*P* = 0.03). In mature bones, the difference is 3.1% (*P* = 0.09). By contrast, averaged mineral content differences are much greater in the 'compression' than in the 'tension' cortex in each age group (immature 8.6%, *P* < 0.001; mature 7.8%, *P* < 0.001).

In immature bones, mineral content of the 'tension' tra-becular tract is not significantly different from the adjacent 'tension' cortex (1.8% difference; *P* = 0.24). By contrast, mineral content of the 'compression' trabecular tract of immature bones tends to be lower than its corresponding 'compression' cortex (3.0% difference; cortical > trabecular; *P* = 0.05).

In mature bones the mineral content of the 'tension' tra-becular tract is not significantly different from the adjacent 'tension' cortex (2.6% difference; *P* = 0.13). By contrast, mineral content of the 'compression' tract of mature bones is markedly lower than its corresponding 'compression' cortex (7.3% difference; cortical > trabecular; *P* < 0.001). This difference, which is greater than that in the immature

bones (3.0% vs. 7.3%), can be partially explained by the combined influences of a small age-related decrease (2.4%) in the 'compression' tract and a small age-related increase (1.7%) in the 'compression' cortex.

Analysis of combined data from both 'tension' and 'compression' regions (40% + 50% trabecular data vs. 40% + 50% cortical data) shows that in skeletally mature bones, cortical bone generally has 5% higher mineral content compared with trabecular bone; there is essentially no difference in the immature bones (< 1.0% greater in cortical bone).

Microscopic mineralization level and heterogeneity data from BSE images

Results of the BSE-image-derived mineralization analyses are summarized in Table 1, and representative images are shown in Figs 3 and 4. The mature and immature bones both showed significant differences in WMGL between the 'compression' and 'tension' trabecular tracts. WMGLs for the standards are: first, 55.80 for MgO ($Z = 10.41$); and second, 103.87 for Al_2O_3 ($Z = 10.65$). With respect to measures of mineralization heterogeneity (FWHM, skewness, and kurtosis), only the immature bones showed significant differences between the 'tension' and 'compression' trabecular tracts. By contrast, the trabecular bone packet prevalence (no. packets/bone area) is significantly greater in the tension tract of only the mature bones.

Table 1 Micromineralization and packet score data and *P*-values in immature (a) and mature (b) bones at their 50% location.

	Dorsal	Plantar	*P*-value
(a) Immature bones (*n* = 7)			
BSE mineral content (WMGL)	135.5 (3.2)	127.1 (3.5)	0.002
Mineral heterogeneity (FWHM of BMDD)	4.8 (0.1)	5.1 (0.2)	0.01
Skewness of BMDD	1.16 (0.0)	1.05 (0.0)	0.007
Kurtosis of BMDD	−0.11 (0.1)	−0.36 (0.1)	0.02
Packet prevalence	46.2 (3.6)*	44.9 (2.8)	ns
(b) Mature bones (*n* = 7)			
BSE mineral content (WMGL)	137.8 (3.7)	128.9 (3.3)	< 0.001
Mineral heterogeneity (FWHM of BMDD)	4.7 (0.1)	4.8 (0.1)	ns
Skewness of BMDD	1.17 (0.0)	1.13 (0.0)	ns
Kurtosis of BMDD	−0.10 (0.0)	−0.20 (0.1)	ns
Packet prevalence	34.6 (2.4) *	48.3 (3.0)	0.006

*Significantly different (*P* < 0.05) from other age group in comparison with the same tract (i.e. dorsal vs. dorsal comparison; or plantar vs. plantar comparison).
ns = non-significant, where all *P* values are > 0.2.
Packet prevalence = no. packets mm^{-2} of bone.
BMDD, bone mineral density distribution; BSE, backscattered electron; FWHM, full-width half-maximum; WMGL, weighted mean gray level.

Micro-CT data

Results of the micro-CT analyses are summarized in Table 2, and representative images are shown in Fig. 5. The mature and immature bones showed significant differences in the DA between 'compression' and 'tension' tracts. The immature bones showed significant differences in BVF and SMI between the 'compression' and 'tension' trabecular tracts. Trends were only shown in the Bs/Bv and Tb.N data, but were not consistent between the groups.

Discussion

Our results do not support our hypothesis that in immature and mature mule deer calcanei, 'compression' trabecular tracts would have significantly elevated mineral content (i.e. percent ash) compared with 'tension' trabecular tracts. In fact, we found only a marginal elevation in 'compression' compared with the 'tension', with a mean difference of $\sim$ 3–3.5% (Fig. 2). Prior studies of skeletally mature mule deer calcanei have shown that the dorsal 'compression' cortex has up to 11% greater mineral content than the opposing plantar 'tension' cortex (Skedros et al. 1994a,b). We therefore speculated that the trabecular tracts that are adjacent and continuous with these cortices would exhibit comparable mechanically important mineralization differences. Increased hemi-osteonal renewal is the likely means for achieving the predicted lower mineral content in the 'tension' tract, and it is expected that a relatively large proportion of younger osteons would produce increased mineralization heterogeneity in this tract.

If our data suggest that it seems unlikely that variations in bulk mineralization would be employed as an important means for adapting the tracts for their different load histories, we suggest three explanations. The first is that trabecular bone can readily accommodate regional differences in mechanical requirements through adjustments in various architectural characteristics via regional differences in the mini-modeling process, which can produce functional adaptation during growth (Keaveny & Hayes, 1993; Parfitt et al. 2000; Tanck et al. 2001; Pontzer et al. 2006; Jee et al. 2007). For example, the significant DA differences shown between the tracts of both age groups, and the significant differences in BVF and SMI in the immature bones, likely have important influences on their mechanical properties, as previously shown for these parameters in bulk tests of bovine and ovine trabecular bone (Goldstein et al. 1993; Goulet et al. 1994; Keaveny et al. 2001; Mittra et al. 2005). The second reason is that the extensive osteon-mediated renewal that is required to maintain lower mineral content in the 'tension' tract would likely be deleterious in trabecular bone because the osteoclastic resorption pits, although transient, would weaken the trabecular struts (Hernandez et al. 2006; Busse et al. 2009; van Oers et al. 2011). The third is that the trabecular bone microarchitecture causes a
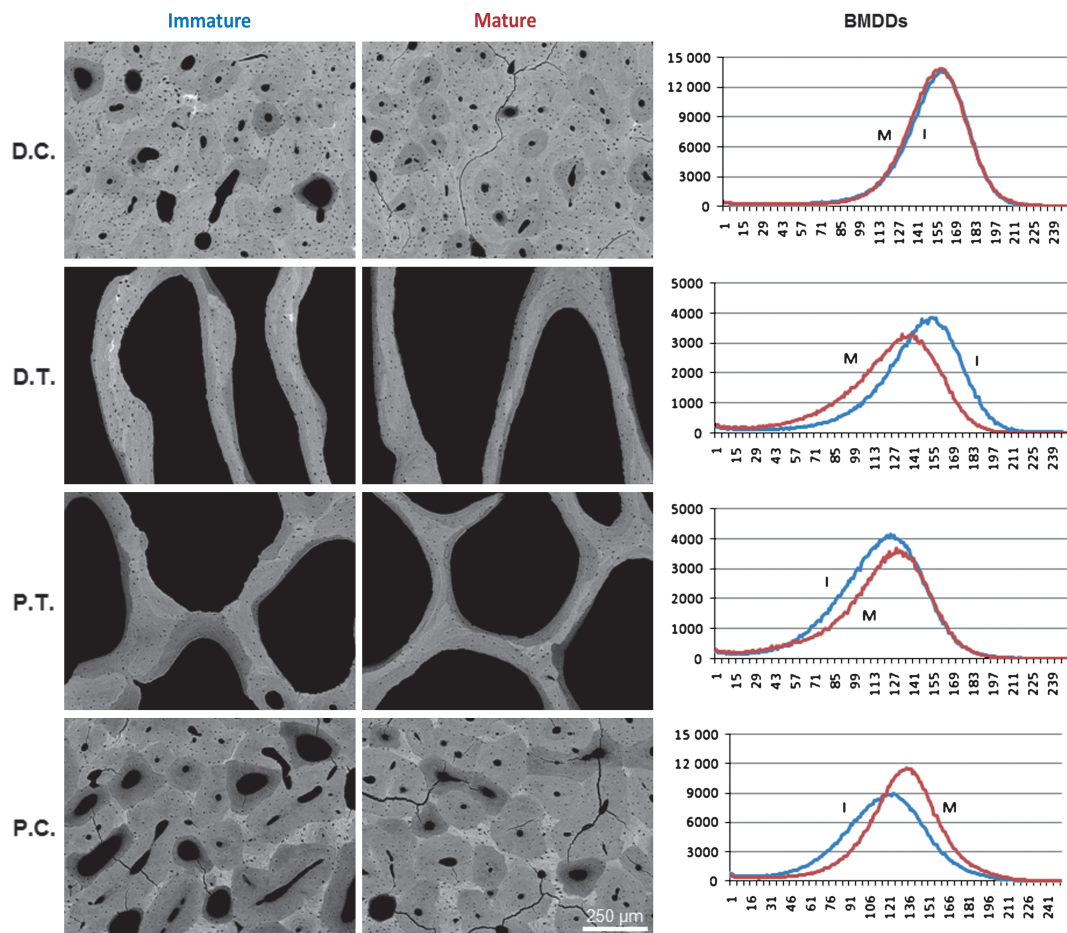
Fig. 3 On the left are BSE images showing differences in gray levels that represent differences in mineral content (Bloebaum et al. 1997). On the right are the gray level profiles for each of the images shown [M = mature (red curve); I = immature (blue curve)]. Mineralization heterogeneity is quantified as the FWHM of the main gray level peak in each of these profiles. The FWHM data reflect bone mineral density distribution (BMDD). Packets, which are the basic structural units typically formed by hemi-osteons, can be distinguished by their differences in mineralization, directions and/or intensity of lamellations (banding patterns), and/or cement lines. Gray level profiles that are shifted more to the right represent increased mineralization. The gray level contrasts in these images are directly comparable because they were obtained in the same imaging session, with the magnification and all other electron beam conditions being identical. D.C., dorsal cortex; D.T., dorsal tract; P.T., planar tract; P.C., planar cortex.

complicated stress distribution. For example, while the region of trabecular bone may be loaded in compression, subregions (individual trabeculae) may be experiencing tension (Bayraktar et al. 2004). In turn the differences in net tension and compression between the respective plantar and dorsal regions are not as distinct as we assume. Even in view of these possibilities, it remains possible that the small mineral content differences could be mechanically important when coupled with one or more trabecular architectural characteristics. This possibility is discussed further below.

Tissue mineralization heterogeneity

Before considering whether the apparently 'minor' mineral content differences derived from percent ash measurements (Fig. 2) are either inconsequential or, in fact, important in a

mechanical context, the reasons why mature calcanei have significant differences between their 'compression' and 'tension' tracts in the BSE-derived mineral content (WMGL) data (but not in percent ash data) should be explained (Table 1). Although not measured in the present study, regional differences in the amount of unmineralized bone (osteoid) that is associated with active mini-modeling during growth can explain the paradox between the BSE-image vs. percent ash data. Because the BSE images only show mineralized bone, the presence of osteoid does not influence the mineral content or mineral heterogeneity (BMDD) measurements made using BSE imaging technology (Boyde et al. 1986). By contrast, osteoid can contribute to producing apparent differences in mineral content when measured in terms of percent ash content. This is because osteoid volume and renewal rates are positively correlated (Martin & Burr, 1989, p. 81), and both of these
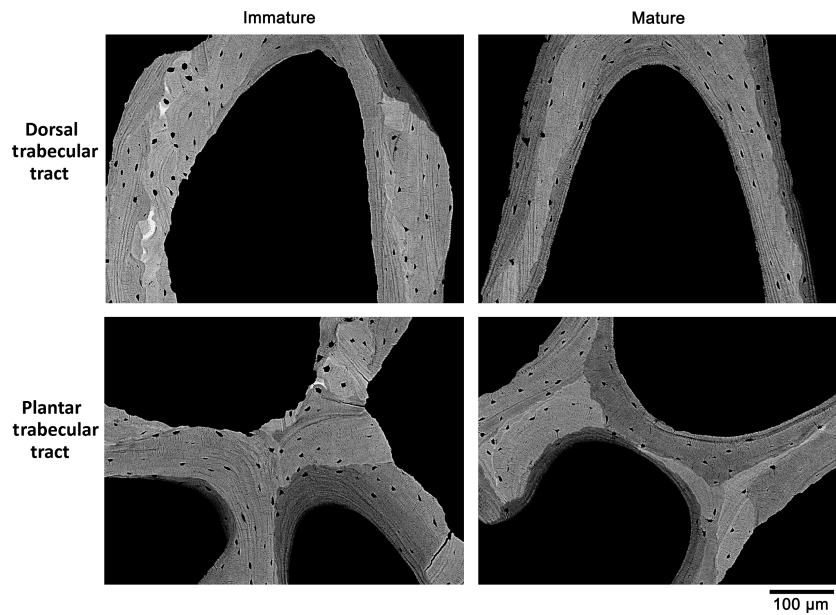
Fig. 4 BSE images of immature and mature deer calcanei at 200 ×. The gray level contrasts in these images are directly comparable because they were obtained in the same imaging session, with the magnification and all other electron beam conditions being identical.

Table 2 Micro-CT data and *P*-values in immature (a) and mature (b) bones at their 50% location.

	Dorsal	Plantar	*P*-value
(a) Immature bones (*n* = 7)			
DA	7.38 (0.70)	4.05 (0.35)	0.01
BVF	0.43 (0.03)	0.58 (0.05)	0.03
Bs∕Bv	11.20 (1.25)*	8.61 (0.85)*	0.07
Tb.Th	0.20 (0.04)*	0.22 (0.03)*	ns
Tb.Sp	0.33 (0.09)	0.23 (0.04)*	ns
Tb.N	2.31 (0.19)*	2.40 (0.14)*	ns
Conn.D	8.84 (1.63)*	7.77 (1.06)*	ns
SMI	−0.40 (0.35)	−3.60 (1.01)	0.02
(b) Mature bones (*n* = 7)			
DA	6.75 (0.83)	3.88 (0.35)	0.02
BVF	0.52 (0.06)	0.56 (0.04)	ns
Bs∕Bv	6.00 (1.23)*	5.62 (0.59)*	ns
Tb.Th	0.47 (0.06)*	0.45 (0.08)*	ns
Tb.Sp	0.84 (0.26)	0.54 (0.05)*	ns
Tb.N	1.30 (0.08)*	1.50 (0.07)*	0.09
Conn.D	1.83 (0.31)*	2.29 (0.15)*	ns
SMI	−2.78 (0.93)	−3.36 (0.68)	ns

*Significantly different (*P* < 0.05) from other age group in comparison with the same tract (i.e. dorsal vs. dorsal comparison; or plantar vs. plantar comparison).
ns = non-significant, where all *P*-values are > 0.2.
Bs∕Bv, bone surface density; BVF, bone value fraction; Conn.D, connectivity density; DA, degree of anisotropy; SMI, structural model index; Tb.N, trabecular number; Tb.Sp, trabecular spacing; Tb.Th, trabecular thickness.

parameters can increase the numerical value of the denominator in the ash fraction ratio, thus lowering mineral content. This may explain the lack of percent ash differences between tracts of mature bones (here a trend was found, *P* = 0.09), even though the BSE image-derived mineral content is significantly different between these regions (*P* < 0.02).

Nano-indentation studies that have shown a strong relationship between variations in local micromineralization and tissue stiffness (Rho et al. 1997; Roy et al. 1999; Zysset et al. 1999; Hoffler et al. 2000; Mulder et al. 2008) support the probability that the mineralization variations obtained from BSE images of our immature bones (BMDD and mineral content) and mature bones (only mineral content) can have important mechanical consequences at a local level (e.g. in a single trabeculum). The presence of significant differences in BMDD between tracts in only the immature bones likely reflects the dual influences of increased mini-modeling and hemi-osteonal remodeling during formation of the 'tension' tract. Qualitative observations suggest that this correlates with differences in the temporal∕spatial maturation of the tracts, where the 'tension' tract lags behind the 'compression' tract (Skedros et al. 2001; Table 1).

The significant mineral content difference shown between the trabecular tracts of mature bones contrasts with data showing that the intra-trabecular mineral distribution is nearly constant in healthy adult humans, and is independent of age, gender, ethnic origin and skeletal site (Roschger et al. 2001; Ruffoni et al. 2007). Roschger et al. (2003, 2008) suggest that the remarkably small biological variance in mineral distribution could reflect the existence of an evolutionary optimum with respect to the biomechanical performance of bone trabeculae. Deviations from a 'normal distribution of mineralization' due to either disease and∕or treatment might therefore be of significant biological and clinical relevance (Roschger et al. 2008;
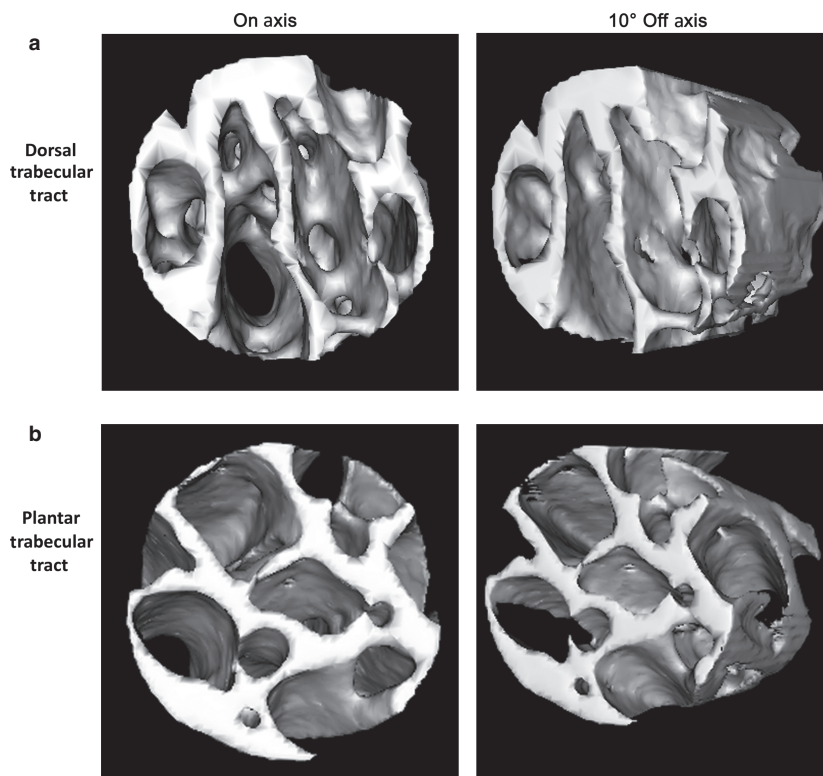
Fig. 5 Three-dimensional reconstructed images obtained from micro-CT scans of the 50% segment of a mature mule deer calcaneus. The views are longitudinal ('on axis') and approximately 10° off axis in the dorsal 'compression' trabecular tract (a) and plantar 'tension' trabecular tract (b). Cylinder diameter = 3 mm.

Renders et al. 2011). It would also be important if plasticity in the 'normal distribution of mineralization' can allow for modifications that differentially adapt trabecular regions for differences in their strain history. We believe that this is what is shown by the significant differences in the data in the mature calcanei shown in Table 1; namely, adaptations for habitual tension vs. compression strain histories. Hence, the idea of a mineral content 'optimum' is not consistent with our data.

Biomechanics of trabecular bone packets

Data supporting the likelihood that the presence, and regional heterogeneity, of trabeculum-level adaptations in deer calcanei are important for resisting/accommodating microdamage formation and propagation include: first, basal levels of microdamage are higher in trabecular than in cortical bone (Schaffler et al. 1995; Fazzalari et al. 1998); and second, the incidence, type and potential for deleterious consequences of microdamage are often dependent on the mode of loading (e.g. tension vs. compression; Reilly et al. 1997; Boyce et al. 1998; Robling et al. 2006). Bone packets (Parfitt, 1979) are therefore an important toughening mechanism in trabecular bone because they create interfaces and potentially increase mineral heterogeneity as a consequence of differences in their mean tissue age (Roschger et al. 2008; Wang et al. 2008; Busse et al. 2009; Smith et al. 2010; Hartmann et al. 2011). Because the bones examined in this study are from wild animals that are not 'old' (none was > 4 years old), it is likely that the increased packet prevalence in the 'tension' tract of mature bones is mechanically beneficial (not a circumstance of senescence or disease). This possibility should be further examined with mechanical testing of bulk specimens and individual trabeculae, and should be contrasted with data reported in normal vs. osteoporotic human trabecular bone because: first, osteoporotic bone has increased packet prevalence and increased BMDD (not found in mature calcanei); and second, changes in material characteristics are correlated with degradations in individual trabeculae for a variety of mechanical properties (stiffness, strength and energy absorption; Busse et al. 2009). By contrast, we suspect that the significantly greater packet prevalence in the 'tension' tract of mature deer calcanei enhances local mechanical competence by being coupled with architectural and/or other material characteristics (Hernandez & Keaveny, 2006).

Cortical vs. trabecular bone mineralization, BVF and mechanical properties

The cortices of immature and mature deer calcanei have, on average, ~ 5% greater mineral content combined than their adjacent trabecular tracts (Fig. 2). Previous studies show that cortical bone has on average about 5–6% greater mineral content than the adjacent trabecular bone (Gong

et al. 1964; Currey, 1988; Hodgskinson et al. 1989).[2] However, using micro-hardness testing of individual trabeculae compared with nearby cortical bone, Hodgskinson et al. (1989) concluded that even with calcium content differences on the order of 10% it is '... unlikely that the Young's modulus of cancellous [trabecular] bone material is much different from that of compact bone.' These data starkly contrast with the significant differences that occur in cortical bone mechanical properties when mineral content differences exceed ∼ 3–4% (Currey, 1969, 1984; Skedros et al. 1994a). The question that must be addressed is whether this small difference affects their mechanical properties?

The few studies that have assessed the influence of tissue (material) density (which is directly and strongly correlated with ash fraction) on the mechanical behavior of bovine and human trabecular bone in bulk testing have shown little, if any, correlation between the level of tissue mineralization with compressive strength (Galante et al. 1970; Behrens et al. 1974; Ducheyne et al. 1977; Turner, 1989). Even the results of studies of Galante et al. (1970) and Turner (1989), which revealed a weak influence of tissue mineral content on mechanical properties of human and bovine trabecular bone in compression, showed that this was linked to variations in apparent density, which explained 88% and 77% of the variance in these tests, respectively, but was not correlated with tissue density.[3] These studies also show that apparent density plays a relatively more important role than trabecular orientation in accommodating differences in local mechanical requirements. In turn, apparent density and trabecular orientation account for ∼ 90% of the variance in the mechanical behaviors of trabecular bone in the loading conditions that have been examined (Goldstein et al. 1993; Goulet et al. 1994; Keaveny et al. 2001; Perilli et al. 2008). But in these studies the variance in tissue mineralization is much smaller than that shown between the two trabecular tracts of our deer calcanei. When tissue mineralization variations are relatively larger, then the influence of tissue mineralization could exceed the influence of BVF on the strength of trabecular bone (Hernandez et al. 2001). Perhaps there is a trend toward this relationship in deer calcanei. Important mechanical behaviors attributable to differences in mineral content, BVF and packet prevalence between the tracts in deer calcanei, and whether or not they are coupled or compensatory, might be revealed by multiple variable regression analyses of mechanically tested bulk specimens. The possibility that this coupling (or compensation) is a means for enhancing bone quality is supported by recent experimental data suggesting that differences in whole bone robusticity are compensated by changes in degree of tissue mineralization (Jepsen, 2011).

Architectural characteristics and potential synergism with material characteristics

The significant BVF difference between the tracts in only the immature bones ($P = 0.03$) could represent residual evidence of a temporal transition from the accumulation of trabecular bone mass in earlier development to the culmination of functional adaptation of trabecular architecture in the later stages of skeletal maturation. This transition has been shown in axial and appendicular bones of growing pigs, and has been described as the progressive emergence of 'a more efficient trabecular structure' (Tanck et al. 2001). Although this transition has not been studied in deer calcanei, our observations suggest that it is also likely reflected in the age-related emergence of generally increased trabecular DA in addition to the dorsal-plantar differences in DA. This difference is similar to that reported between the DA of superior 'tension' and inferior 'compression' trabecular tracts of human femoral necks (Lai et al. 2005).

It is possible that the trend toward increased trabecular number (Tb.N) in the plantar cortex of mature bones ($P = 0.09$; Table 2) also reflects functional adaptation with development. Although it might be expected that this parameter is linked to a dorsal-plantar BVF difference, this relationship is only demonstrated in mature calcanei. A study of interrelationships of trabecular mechanical properties and microstructural characteristics in femoral trabecular bone of mature sheep showed that SMI and BVF correlated with Tb.Th and Tb.Sp, and less with Tb.N and Conn.D (Mittra et al. 2005). Therefore, an increase in BVF results in an increase in Tb.Th, but may not cause an increase in Tb.N or Conn.D. Tb.N and Conn.D could be adaptive even when not closely linked to BVF, SMI, Tb.Th and Tb.Sp.

Our qualitative observations made with a magnifying lens revealed what appeared to be trabeculae that are plate-like in some regions and rod-like in others. In view of this observation and data from Mittra et al. (2005) in mature sheep femora showing that trabecular rod- vs. plate-like morphology (i.e. SMI data) strongly correlate with mechanical properties of bulk trabecular specimens, we hypothesized that SMI data would differ between the tracts. However, our data showed that this only occurred in the immature bones ($P = 0.02$), where the dorsal vs. plantar difference is in the degree of 'honeycomb-like shapes' of the trabeculae (i.e. there is no rod vs. plate difference).

---

[2]Tassani et al. (2011) did not find this difference in their tissue mineralization data (based on ashing and bone volume) from trabecular and cortical bone specimens from adult human tibiae and femora. In addition to species influences, this discrepancy might reflect different methodologies: first, adjacent cortical and trabecular samples were not compared; and second specimen porosity may have been determined imprecisely.

[3]Apparent density is typically expressed as the mass of tissue ÷ bulk volume of the specimen; this parameter is a close approximation of BVF because bone tissue density is typically constant in the bone specimens where this relationship has been examined (Carter & Hayes, 1977; Rice et al. 1988; Hernandez et al. 2001; Tassani et al. 2011).

Consequently, we did not identify a trabecular architectural characteristic that clearly correlates with habitual compression or tension loading.

Study limitations

One important limitation of this study is that the 'tension' and 'compression' trabecular tracts cannot function independently because they are highly interconnected, especially in the distal calcaneal shaft (Fig. 1). Although we sampled bone in regions where the tracts appear to become independent when viewed in lateral radiographs, this confounding issue cannot be eliminated. Additionally, it is possible that strains measured on the surface of a bone might not closely reflect the magnitudes and/or distributions of the strains produced in the deeper trabecular bone (Bay et al. 1999; Keaveny et al. 2001; Van Rietbergen et al. 2003; Renders et al. 2006). We know of no evidence supporting or rejecting the assumption that the dorsal and plantar tracts actually experience a different and habitually prevalent/predominant strain mode. But the lack of some correspondence of the trabecular tracts with principal stresses/strains would be unexpected. If this were the case, it would invalidate this model as a 'good example' of Wolff's trajectorial theory of trabecular bone architectural adaptation (Lanyon, 1974; Skedros & Baucom, 2007). Trabecular bone also contributes to the cross-sectional geometric properties along a majority of the calcaneal shaft. For example, Ruff (1983) has suggested that the contribution of trabecular bone to the structural properties of a diaphyseal region becomes important when this type of bone occupies more than ∼ 40% of the total cross-sectional area. Trabecular bone exceeds this percentage over nearly 60% of shaft length (Skedros et al. 1994a). Consequently, a complete biomechanical analysis of cross-sectional geometric properties of the deer calcaneus must avoid considering contributions from cortical or trabecular bone in isolation, especially in view of the highly asymmetric cortical distribution (i.e. greater mass in the 'compression' cortex; Fox & Keaveny, 2001; Bhatavadekar et al. 2006; Holzer et al. 2009).

Summary and conclusions

We found small tissue mineral content (percent ash) differences between bulk specimens of the trabecular tracts that are only statistically significant in the immature bones where growth-related modeling dynamics are still present. Mechanical testing studies of human and bovine trabecular bone suggest that these small (percent ash) differences are not mechanically important when considered independently of other architectural and material characteristics – at least not in the contexts of the conventional mechanical tests that have been conducted in other artiodactyl species and humans. In this perspective it could be concluded that if local adaptations are required in the 'tension' and 'com-

pression' trabecular tracts of the mule deer calcaneus, then this is more readily achieved through architectural modifications. However, it is possible that unrecognized and biomechanically important synergisms exist between tissue mineralization (shown to be statistically significant between dorsal and plantar tracts in both age groups in the BSE image analysis), packet prevalence (shown only in mature bones) and/or trabecular micro-architecture (both age groups). These postulated relationships might reveal the potential for adaptive plasticity and biomechanical interactions of mini-modeling and hemi-osteonal renewal activities that has not been recognized – because prior studies have not been able to isolate strain histories where this might be at work. Additional studies are also needed to more firmly establish the presumed *in vivo* strain distributions of this model, and the strengths and weaknesses of using it for drawing comparisons with more complexly loaded bones that are also thought to have significant bending during their normal use, including the human femoral neck.

Acknowledgments

References

Anderson AE (1981) Morphologic and Physiological Characteristics. In: *Mule and Black-Tailed Deer of North America*, Chapter 2, pp. 27–97. Lincoln, NE: University of Nebraska Press.

Banks WJ, Glenwood PE, Kainer RA (1968) Antler growth and osteoporosis: morphological and morphometric changes in the costal compacta during the antler growth cycle. *Anat Rec*, **162**, 387–398.

Barak MM, Lieberman DE, Hublin JJ (2011) A Wolff in sheep's clothing: trabecular bone adaptation in response to changes in joint loading orientation. *Bone*, **49**, 1141–1151.

Bay BK, Yerby SA, McLain RF, et al. (1999) Measurement of strain distributions within vertebral body sections by texture correlation. *Spine (Phila Pa 1976)*, **24**, 10–17.

Bayraktar HH, Morgan EF, Niebur GL, et al. (2004) Comparison of the elastic and yield properties of human femoral trabecular and cortical bone tissue. *J Biomech*, **37**, 27–35.

Behrens JC, Walker PS, Shoji H (1974) Variations in strength and structure of cancellous bone at the knee. *J Biomech*, **7**, 201–207.

Bhatavadekar NB, Daegling DJ, Rapoff AJ (2006) Application of an image-based weighted measure of skeletal bending stiffness to great ape mandibles. *Am J Phys Anthropol*, **131**, 243–251.

Biewener AA, Bertram JEA (1993) Mechanical loading and bone growth *in vivo*. In: *Bone, Volume 7, Bone Growth – B* (ed. Hall BK), pp. 1–36. Boca Raton, FL: CRC Press.

Biewener AA, Fazzalari NL, Konieczynski DD, et al. (1996) Adaptive changes in trabecular architecture in relation to functional strain patterns and disuse. *Bone*, **19**, 1–8.

Bloebaum RD, Skedros JG, Vajda EG, et al. (1997) Determining mineral content variations in bone using backscattered electron imaging. *Bone*, **20**, 485–490.

Bloebaum RD, Lundeen GA, Shea JE, et al. (2004) Age-related mineralization heterogeneity changes in trabecular bone of the proximal femur. *Anat Rec A Discov Mol Cell Evol Biol*, **281**, 1296–1302.

Boskey AL (2001) Bone mineralization. In: *Bone Mechanics Handbook* (ed. Cowin SC), pp. 5-1–5-33. Boca Raton, FL: CRC Press.

Boskey AL, Spevak L, Weinstein RS (2009) Spectroscopic markers of bone quality in alendronate-treated postmenopausal women. *Osteoporos Int*, **20**, 793–800.

Bousson V, Meunier A, Bergot C, et al. (2001) Distribution of intracortical porosity in human midfemoral cortex by age and gender. *J Bone Miner Res*, **16**, 1308–1317.

Bousson V, Bergot C, Wu Y, et al. (2011) Greater tissue mineralization heterogeneity in femoral neck cortex from hip-fractured females than controls. A microradiographic study. *Bone* **48**, 1252–1259.

Boyce TM, Fyhrie DP, Glotkowski MC, et al. (1998) Damage type and strain mode associations in human compact bone bending fatigue. *J Orthop Res*, **16**, 322–329.

Boyde A, Maconnachie E, Reid SA, et al. (1986) Scanning electron microscopy in bone pathology: review of methods, potential and applications. *Scan Electron Microsc*, **4**, 1537–1554.

Busse B, Hahn M, Soltau M, et al. (2009) Increased calcium content and inhomogeneity of mineralization render bone toughness in osteoporosis: mineralization, morphology and biomechanics of human single trabeculae. *Bone*, **45**, 1034–1043.

Carter DR, Hayes WC (1977) The compressive behavior of bone as a two-phase porous structure. *J Bone Joint Surg Am*, **59**, 954–962.

Ciarelli TE, Fyhrie DP, Parfitt AM (2003) Effects of vertebral bone fragility and bone formation rate on the mineralization levels of cancellous bone from white females. *Bone*, **32**, 311–315.

Ciarelli TE, Tjhia C, Rao DS, et al. (2009) Trabecular packet-level lamellar density patterns differ by fracture status and bone formation rate in white females. *Bone*, **45**, 903–908.

Currey JD (1969) The mechanical consequences of variation in the mineral content of bone. *J Biomech*, **2**, 1–11.

Currey JD (1984) *The Mechanical Adaptations of Bones*. Princeton, NJ: Princeton University Press.

Currey JD (1988) The effect of porosity and mineral content on the Young's modulus of elasticity of compact bone. *J Biomech*, **21**, 131–139.

Ding M, Hvid I (2000) Quantification of age-related changes in the structure model type and trabecular thickness of human tibial cancellous bone. *Bone*, **26**, 291–295.

Ducheyne P, Heymans L, Martens M, et al. (1977) The mechanical behaviour of intracondylar cancellous bone of the femur at different loading rates. *J Biomech*, **10**, 747–762.

Emmanual J, Hornbeck C, Bloebaum RD (1987) A polymethyl methacrylate method for large specimens of mineralized bone with implants. *Stain Tech*, **62**, 401–410.

Fajardo RJ, Muller R (2001) Three-dimensional analysis of nonhuman primate trabecular architecture using micro-computed tomography. *Am J Phys Anthropol*, **115**, 327–336.

Fajardo RJ, Muller R, Ketcham RA, et al. (2007) Nonhuman anthropoid primate femoral neck trabecular architecture and its relationship to locomotor mode. *Anat Rec (Hoboken)*, **290**, 422–436.

Fazzalari NL, Forwood MR, Smith K, et al. (1998) Assessment of cancellous bone quality in severe osteoarthrosis: bone mineral density, mechanics, and microdamage. *Bone*, **22**, 381–388.

Follet H, Boivin G, Rumelhart C, et al. (2004) The degree of mineralization is a determinant of bone strength: a study on human calcanei. *Bone*, **34**, 783–789.

Fox JC, Keaveny TM (2001) Trabecular eccentricity and bone adaptations. *J Theor Biol*, **212**, 211–221.

Fritton SP, Rubin CT (2001) *In vivo* measurement of bone deformations using strain gauges. In: *Bone Biomechanics Handbook* (ed. Cowin SC), pp. 8-1–8-41. Boca Raton, FL: CRC Press.

Galante J, Rostoker W, Ray RD (1970) Physical properties of trabecular bone. *Calcif Tissue Res*, **5**, 236–246.

Goldstein SA, Goulet R, McCubbrey D (1993) Measurement and significance of three-dimensional architecture to the mechanical integrity of trabecular bone. *Calcif Tissue Int*, **53** (Suppl 1), S127–S132. discussion S132–S133.

Gong JK, Arnold JS, Cohn SH (1964) Composition of trabecular and cortical bone. *Anat Rec*, **149**, 325–331.

Goss RJ (1983) *Deer Antlers. Regeneration, Function, and Evolution*. New York, NY: Academic Press.

Goulet RW, Goldstein SA, Ciarelli MJ, et al. (1994) The relationship between the structural and orthogonal compressive properties of trabecular bone. *J Biomech*, **27**, 375–389.

Gunasekaran B, Constantz BR, Monjazeb M, et al. (1991) An effective way of assessing crosslinks of collagenous proteins in biomaterials and tissues. *Trans Soc Biomaterials*, **XIV**, 139.

Hartmann MA, Dunlop JW, Brechet YJ, et al. (2011) Trabecular bone remodelling simulated by a stochastic exchange of discrete bone packets from the surface. *J Mech Behav Biomed Mater*, **4**, 879–887.

Hernandez CJ, Keaveny TM (2006) A biomechanical perspective on bone quality. *Bone*, **39**, 1173–1181.

Hernandez CJ, Beaupre GS, Keller TS, et al. (2001) The influence of bone volume fraction and ash fraction on bone strength and modulus. *Bone*, **29**, 74–78.

Hernandez CJ, Gupta A, Keaveny TM (2006) A biomechanical analysis of the effects of resorption cavities on cancellous bone strength. *J Bone Miner Res*, **21**, 1248–1255.

Hildebrand T, Ruegsegger P (1997) A new method for the model-independent assessment of thickness in three-dimensional images. *J Microsc*, **185**, 67–75.

Hildebrand T, Laib A, Muller R, et al. (1999) Direct three-dimensional morphometric analysis of human cancellous bone: microstructural data from spine, femur, iliac crest, and calcaneus. *J Bone Miner Res*, **14**, 1167–1174.

Hill CA, Richtsmeier JT (2008) A quantitative method for the evaluation of three-dimensional structure of temporal bone pneumatization. *J Hum Evol*, **55**, 682–690.

Hillman JR, Davis RW, Abdelbaki YZ (1973) Cyclic bone remodeling in deer. *Calcif Tissue Res*, **12**, 323–330.

Hintze J (1995) *Number Cruncher Statistical Systems 6.0 User's Manual*. Kaysville, Utah: Number Cruncher Statistical Systems.

Hodgkinson R, Currey JD, Evans GP (1989) Hardness, an indicator of the mechanical competence of cancellous bone. *J Orthop Res*, **7**, 754–758.

Hoffler CE, Moore KE, Kozloff K, et al. (2000) Heterogeneity of bone lamellar-level elastic moduli. *Bone*, **26**, 603–609.

Holzer G, von Skrbensky G, Holzer LA, et al. (2009) Hip fractures and the contribution of cortical versus trabecular bone to femoral neck strength. *J Bone Miner Res*, **24**, 468–474.

Jee WS, Tian XY, Setterberg RB (2007) Cancellous bone minimodeling-based formation: a Frost, Takahashi legacy. *J Musculoskelet Neuronal Interact*, **7**, 232–239.

Jepsen KJ (2011) Functional interactions among morphologic and tissue quality traits define bone quality. *Clin Orthop Relat Res*, **469**, 2150–2159.

Keaveny TM, Hayes WC (1993) Mechanical properties of cortical and trabecular bone. In: *Bone* (ed. Hall BK), pp. 285–344. Boca Raton, FL: CRC Press.

Keaveny TM, Guo XE, Wachtel EF, et al. (1994a) Trabecular bone exhibits fully linear elastic behavior and yields at low strains. *J Biomech*, **27**, 1127–1136.

Keaveny TM, Wachtel EF, Ford CM, et al. (1994b) Differences between the tensile and compressive strengths of bovine tibial trabecular bone depend on modulus. *J Biomech*, **27**, 1137–1146.

Keaveny TM, Morgan EF, Niebur GL, et al. (2001) Biomechanics of trabecular bone. *Annu Rev Biomed Eng*, **3**, 307–333.

Ketcham RA, Ryan TM (2004) Quantification and visualization of anisotropy in trabecular bone. *J Microsc*, **213**, 158–171.

Kreider JM, Goldstein SA (2009) Trabecular bone mechanical properties in patients with fragility fractures. *Clin Orthop Relat Res*, **467**, 1955–1963.

Lai YM, Qin L, Yeung HY, et al. (2005) Regional differences in trabecular BMD and micro-architecture of weight-bearing bone under habitual gait loading – a pQCT and microCT study in human cadavers. *Bone*, **37**, 274–282.

Lanyon LE (1974) Experimental support for the trajectorial theory of bone structure. *J Bone Joint Surg*, **56B**, 160–166.

Lanyon LE, Baggott DG (1976) Mechanical function as an influence on the structure and form of bone. *J Bone Joint Surg*, **58-B**, 436–443.

Lieberman DE, Polk JD, Demes B (2004) Predicting long bone loading from cross-sectional geometry. *Am J Phys Anthropol*, **123**, 156–171.

Loveridge N, Power J, Reeve J, et al. (2004) Bone mineralization density and femoral neck fragility. *Bone*, **35**, 929–941.

MacLatchy L, Muller R (2002) A comparison of the femoral head and neck trabecular architecture of Galago and Perodicticus using micro-computed tomography (microCT). *J Hum Evol*, **43**, 89–105.

Maga M, Kappelman J, Ryan TM, et al. (2006) Preliminary observations on the calcaneal trabecular microarchitecture of extant large-bodied hominoids. *Am J Phys Anthropol*, **129**, 410–417.

Martin RB, Burr DB (1989) *Structure, Function and Adaptation of Compact Bone*. New York, NY: Raven Press.

Mittra E, Rubin C, Qin YX (2005) Interrelationship of trabecular mechanical and microstructural properties in sheep trabecular bone. *J Biomech*, **38**, 1229–1237.

Moreno CA, Main RP, Biewener AA (2008) Variability in forelimb bone strains during non-steady locomotor activities in goats. *J Exp Biol*, **211**, 1148–1162.

Mulder L, Koolstra JH, den Toonder JM, et al. (2008) Relationship between tissue stiffness and degree of mineralization of developing trabecular bone. *J Biomed Mater Res A*, **84**, 508–515.

Muller R, Van Campenhout H, Van Damme B, et al. (1998) Morphometric analysis of human bone biopsies: a quantitative structural comparison of histological sections and micro-computed tomography. *Bone*, **23**, 59–66.

Odgaard A, Kabel J, van Rietbergen B, et al. (1997) Fabric and elastic principal directions of cancellous bone are closely related. *J Biomech*, **30**, 487–495.

van Oers RF, van Rietbergen B, Ito K, et al. (2011) Simulations of trabecular remodeling and fatigue: is remodeling helpful or harmful? *Bone*, **48**, 1210–1215.

Parfitt AM (1979) Quantum concept of bone remodeling and turnover: implications for the pathogenesis of osteoporosis. *Calcif Tissue Int*, **28**, 1–5.

Parfitt AM, Travers R, Rauch F, et al. (2000) Structural and cellular changes during bone growth in healthy children. *Bone*, **27**, 487–494.

Perilli E, Baleani M, Ohman C, et al. (2008) Dependence of mechanical compressive strength on local variations in microarchitecture in cancellous bone of proximal human femur. *J Biomech*, **41**, 438–446.

Pontzer H, Lieberman DE, Momin E, et al. (2006) Trabecular bone in the bird knee responds with high sensitivity to changes in load orientation. *J Exp Biol*, **209**, 57–65.

Purdue JR (1983) Epiphyseal closure in white-tailed deer. *J Wildl Manage*, **47**, 1207–1213.

Reilly DT, Burstein AH (1975) The elastic and ultimate properties of compact bone tissue. *J Biomech*, **8**, 393–405.

Reilly GC, Currey JD, Goodship A (1997) Exercise of young thoroughbred horses increases impact strength of the third metacarpal bone. *J Orthop Res*, **15**, 862–868.

Renders GA, Mulder L, van Ruijven LJ, et al. (2006) Degree and distribution of mineralization in the human mandibular condyle. *Calcif Tissue Int*, **79**, 190–196.

Renders GA, Mulder L, Langenbach GE, et al. (2008) Biomechanical effect of mineral heterogeneity in trabecular bone. *J Biomech*, **41**, 2793–2798.

Renders GA, Mulder L, van Ruijven LJ, et al. (2011) Mineral heterogeneity affects predictions of intratrabecular stress and strain. *J Biomech*, **44**, 402–407.

Rho JY, Tsui TY, Pharr GM (1997) Elastic properties of human cortical and trabecular lamellar bone measured by nanoindentation. *Biomaterials*, **18**, 1325–1330.

Rice JC, Cowin SC, Bowman JA (1988) On the dependence of the elasticity and strength of cancellous bone on apparent density. *J Biomech*, **21**, 155–168.

Ridler TW, Calvard S (1878) Picture thresholding using an iterative selection method. *IEEE Trans Systems, Man Cybernetics*, **SMC-8**, 630.

Robling AG, Castillo AB, Turner CH (2006) Biomechanical and molecular regulation of bone remodeling. *Annu Rev Biomed Eng*, **8**, 455–498.

Roschger P, Fratzl P, Eschberger J, et al. (1998) Validation of quantitative backscattered electron imaging for the measurement of mineral density distribution in human bone biopsies. *Bone*, **23**, 319–326.

Roschger P, Rinnerthaler S, Yates J, et al. (2001) Alendronate increases degree and uniformity of mineralization in cancellous bone and decreases the porosity in cortical bone of osteoporotic women. *Bone*, **29**, 185–191.

Roschger P, Gupta HS, Berzlanovich A, et al. (2003) Constant mineralization density distribution in cancellous human bone. *Bone*, **32**, 316–323.

Roschger P, Paschalis EP, Fratzl P, et al. (2008) Bone mineralization density distribution in health and disease. *Bone*, **42**, 456–466.

Roy ME, Rho JY, Tsui TY, et al. (1999) Mechanical and morphological variation of the human lumbar vertebral cortical and trabecular bone. *J Biomed Mater Res*, **44**, 191–197.

Ruff CB (1983) The contribution of cancellous bone to long bone strength and rigidity. *Am J Phys Anthrop*, **61**, 141–143.

Ruffoni D, Fratzl P, Roschger P, et al. (2007) The bone mineralization density distribution as a fingerprint of the mineralization process. *Bone*, **40**, 1308–1319.

Ryan TM, Ketcham RA (2002) Femoral head trabecular bone structure in two omomyid primates. *J Hum Evol*, **43**, 241–263.

Ryan TM, Walker A (2010) Trabecular bone structure in the humeral and femoral heads of anthropoid primates. *Anat Rec (Hoboken)*, **293**, 719–729.

Schaffler MB, Choi K, Milgrom C (1995) Aging and matrix microdamage accumulation in human compact bone. *Bone*, **17**, 521–525.

Skedros JG (2011) Interpreting load history in limb-bone diaphyses: important considerations and their biomechanical foundations. In: *Bone Histology: An Anthropological Perspective* (eds Crowder C, Stout S), pp. 385. Boca Raton, FL: CRC Press.

Skedros JG, Baucom SL (2007) Mathematical analysis of trabecular 'trajectories' in apparent trajectorial structures: the unfortunate historical emphasis on the human proximal femur. *J Theor Biol*, **244**, 15–45.

Skedros JG, Brand RA (2011) Biographical sketch: Georg Hermann von Meyer (1815–1892). *Clin Orthop Relat Res*, **469**, 3072–3076.

Skedros JG, Bloebaum RD, Bachus KN, et al. (1993a) The meaning of graylevels in backscattered electron images of bone. *J Biomed Mater Res*, **27**, 47–56.

Skedros JG, Bloebaum RD, Bachus KN, et al. (1993b) Influence of mineral content and composition on graylevels in backscattered electron images of bone. *J Biomed Mater Res*, **27**, 57–64.

Skedros JG, Bloebaum RD, Mason MW, et al. (1994a) Analysis of a tension/compression skeletal system: possible strain-specific differences in the hierarchical organization of bone. *Anat Rec*, **239**, 396–404.

Skedros JG, Mason MW, Bloebaum RD (1994b) Differences in osteonal micromorphology between tensile and compressive cortices of a bending skeletal system: indications of potential strain-specific differences in bone microstructure. *Anat Rec*, **239**, 405–413.

Skedros JG, Chow F, Patzakis MJ (1995) The artiodactyl calcaneus as a model for examining mechanisms governing regional differences in remodeling activities in cortical bone. *J Bone Miner Res*, **10**, S441.

Skedros JG, Su SC, Bloebaum RD (1997) Biomechanical implications of mineral content and microstructural variations in cortical bone of horse, elk, and sheep calcanei. *Anat Rec*, **249**, 297–316.

Skedros JG, Mason MW, Bloebaum RD (2001) Modeling and remodeling in a developing artiodactyl calcaneus: a model for evaluating Frost's mechanostat hypothesis and its corollaries. *Anat Rec*, **263**, 167–185.

Skedros JG, Hunt KJ, Bloebaum RD (2004) Relationships of loading history and structural and material characteristics of bone: development of the mule deer calcaneus. *J Morphol*, **259**, 281–307.

Skedros JG, Holmes JL, Vajda EG, et al. (2005) Cement lines of secondary osteons in human bone are not mineral-deficient: new data in a historical perspective. *Anat Rec A Discov Mol Cell Evol Biol*, **286**, 781–803.

Skedros JG, Sorenson SM, Takano Y, et al. (2006) Dissociation of mineral and collagen orientations may differentially adapt compact bone for regional loading environments: results from acoustic velocity measurements in deer calcanei. *Bone*, **39**, 143–151.

Skedros JG, Sorenson SM, Hunt KJ, et al. (2007) Ontogenetic structural and material variations in ovine calcanei: a model for interpreting bone adaptation. *Anat Rec*, **290**, 284–300.

Skedros JG, Mendenhall SD, Kiser CJ, et al. (2009) Interpreting cortical bone adaptation and load history by quantifying osteon morphotypes in circularly polarized light images. *Bone*, **44**, 392–403.

Skedros JG, Sybrowsky CL, Anderson WE, et al. (2011) Relationships between in vivo microdamage and the remarkable regional material and strain heterogeneity of cortical bone of adult deer, elk, sheep and horse calcanei. *J Anat*, **219**, 722–733.

Smith LJ, Schirer JP, Fazzalari NL (2010) The role of mineral content in determining the micromechanical properties of discrete trabecular bone remodeling packets. *J Biomech*, **43**, 3144–3149.

Sokal RR, Rohlf FJ (1995) *Biometry. The Principles and Practice of Statistics in Biological Research*, 3rd edn. New York, NY: W.H. Freeman.

Stauber M, Muller R (2006) Volumetric spatial decomposition of trabecular bone into rods and plates – a new method for local bone morphometry. *Bone*, **38**, 475–484.

Su SC (1998) Microstructure and mineral content correlations to strain parameters in cortical bone of the artiodactyl calcaneus. In: *Department of Bioengineering (Masters Thesis)*, pp. 64. Salt Lake City, UT: University of Utah.

Su SC, Skedros JG, Bachus KN, et al. (1999) Loading conditions and cortical bone construction of an artiodactyl calcaneus. *J Exp Biol*, **202** (Pt 22), 3239–3254.

Tanck E, Homminga J, van Lenthe GH, et al. (2001) Increase in bone volume fraction precedes architectural adaptation in growing bone. *Bone*, **28**, 650–654.

Tassani S, Ohman C, Baruffaldi F, et al. (2011) Volume to density relation in adult human bone tissue. *J Biomech*, **44**, 103–108.

Trussell HJ (1979) Comments on ''Picture thresholding using an iterative selection method''. *IEEE Trans Systems, Man Cybernetics*, **SMC-9**, 311.

Turner CH (1989) Yield behavior of bovine cancellous bone. *J Biomech Eng*, **111**, 256–260.

Van Rietbergen B, Huiskes R, Eckstein F, et al. (2003) Trabecular bone tissue strains in the healthy and osteoporotic human femur. *J Bone Miner Res*, **18**, 1781–1788.

Wang X, Niebur GL (2006) Microdamage propagation in trabecular bone due to changes in loading mode. *J Biomech*, **39**, 781–790.

Wang X, Sudhaker Rao D, Ajdelsztajn L, et al. (2008) Human iliac crest cancellous bone elastic modulus and hardness differ with bone formation rate per bone surface but not by existence of prevalent vertebral fracture. *J Biomed Mater Res B Appl Biomater*, **85**, 68–77.

Weinkamer R, Fratzl P (2011) Mechanical adaptation of biological materials – the examples of bone and wood. *Mater Sci Eng C*, **31**, 1164–1173.

Zysset PK, Guo XE, Hoffler CE, et al. (1999) Elastic modulus and hardness of cortical and trabecular bone lamellae measured by nanoindentation in the human femur. *J Biomech*, **32**, 1005–1012.